Acta Physiologiae Plantarum (2024) 46:33
https://doi.org/10.1007/s11738-024-03663-7

ORIGINAL ARTICLE

Cell division and dynamics in global DNA methylation associated with radicle protrusion in *Trichocline catharinensis* seeds (Asteraceae)

Ana P. Lando[1] · Daniela Goeten[1] · W. G. Viana[1] · Yohan Fritsche[2] · Miguel P. Guerra[2] · N. Steiner[1]

Received: 1 April 2022 / Revised: 1 February 2024 / Accepted: 8 February 2024 / Published online: 27 February 2024

Abstract

Considering that Asteraceae is an important plant family, we have identified a valuable opportunity to study seed germination a wild species of this family, *Trichocline catharinensis*. Seed germination involves many factors for a transition from low-energy metabolism to a growing seedling. Our understanding of changes of DNA methylation, chromatin structure, and cell cycle activity prior to root protrusion are more limited. Our study allows observed these changes, in the three stages of germination, when it is the promoted by gibberellic acid (GA), or fluridone (FLU) inhibitor of ABA synthesis, or when the process is not succeeded by paclobutrazol (PAC) inhibitor of GA synthesis. Ultrastructural analysis showed cell vacuolization in the hypocotyl-radicle axis by the transformation of protein storage vacuoles to vacuoles, which occurred prior to the initiation of cell elongation. Compacted chromatin in electron-dense regions (heterochromatin) was observed in the mature seeds, becoming loosened during germination in regions of euchromatin. It was identified cells with replicated 4C DNA content (G2 phase of cell cycle) before radicle protrusion, when the reduction of global DNA methylation (GDM) occurs, and DNA replication is possibly initiated. These observations suggest, cell division activation has been to precede radicle protrusion, initiated between phases I and II. When germination is inhibited by PAC, the levels of GDM decreased dramatically in phase III. The results provide information which are necessary for agronomically important practices, such as seed priming. Furthermore, raise to a biological groundwork for future studies looking for use and conservation of biodiversity.

Keywords Cell elongation · Epigenetics · Protein storage vacuoles · Cell cycle · Chromatin · Wild species

Introduction

Trichocline catharinensis (Cabrera) is a Brazilian endemic Asteraceae (Cabrera et al. 1973). It is considered a species of potential economic value due to its rusticity and ornamental characteristics, which have encouraged the use of this species in plant breeding programs, as an ornamental crop, and in ecological programs for ecosystem recovery (Long et al. 2015; Manning et al. 2016). The knowledge about seed behavior is fundamental to the use of native species in ornamental crops and ecological programs for ecosystem recovery (Engelmann 2011), since germination is a crucial step in the establishment of the seedling (Derek Bewley et al. 2012). In addition, seed biology is a major research topic of importance for food security and climate change (Nonogaki 2017; Penfield and MacGregor 2017).

Seed germination is a complex process and we need to understand the underlying molecular, hormonal, and morphological aspects (Steinbrecher and Leubner-Metzger 2018). At maturity, a typical angiosperm diaspore (seed/fruit) consists of an embryo and seed coat, which might include living endosperm, exotesta (seed coat derived from the outer integument) and pericarp (fruit coat) (Steinbrecher and Leubner-Metzger 2018). Quiescent seeds are characterized by an absence of hormone-controlled dormancy and their germination can simply be triggered by imbibition (Weitbrecht et al. 2011; Obroucheva et al. 2017). Thus, the seed germination begins with uptake of water and ends with emergence of the embryonic axis through its surrounding

Communicated by J. Zhao.

✉ N. Steiner
neusa.steiner@ufsc.br

[1] Plant Physiology Laboratory, Department of Botany, Federal University of Santa Catarina, Florianópolis, SC 88040-900, Brazil

[2] Plant Developmental Physiology and Genetics Laboratory, Department of Plant Science, Federal University of Santa Catarina, Florianópolis, SC 88034-001, Brazil

structures (Derek Bewley et al. 2012). An essential event for the completion of germination sensu stricto is elongation of specific cells to result in radicle protrusion (Rewers and Sliwinska 2014; Novikova et al. 2014). Whereas cell elongation is a fundamental process during early seed germination, the initiation of cell division varies between species and can occur simultaneously with elongation or later on (Obroucheva et al. 2012). The cell division is generally considered to occur only at the completion of germination (Derek Bewley et al. 2012). However, in germinating seeds of certain species such as Nicotiana, Solanum, and Arabidopsis, cell division activation has been found to precede radicle protrusion (Masubelele et al. 2005). Flow cytometric analysis of the cell cycle in different parts of the embryo during imbibition has allowed verification of where, and at which phase of germination, DNA synthesis occurs (Sliwinska et al. 2009). Studies using flow cytometry have demonstrated that DNA replication is initiated in the radicle tip cells during hydro-or osmopriming of seeds of Capsicum (Saracco et al. 1995) and *Beta vulgaris* (Lukaszewska et al. 2012).

DNA replication is related to reduction of global DNA methylation (GDM) (Zluvova et al. 2001). DNA methylation generally refers to an addition of a methyl group onto the C5 position of cytosine to form 5-methylcytosine (5mC) (Bird 2002). DNA methylation was studied in wheat seeds during germination and a rapid reduction of global DNA methylation levels was observed in connection with increasing metabolic activity (Drozhdeniuk et al. 1976). Similar results were reported (Zluvova et al. 2001) where a rapid decrease in GDM levels was reported during the germination of *Silene latifolia* seeds, and this event occurred before cell division had begun. Changes in the spatial distribution of DNA methylated sequences are accompanied by changes in chromatin organization (van Zanten et al. 2011). Several authors reported that the highly compacted seed chromatin becomes loosened during germination (Bartels et al. 2018). The chromatin compaction in Arabidopsis seeds quickly decreases upon imbibition (van Zanten et al. 2013). Integrating molecular, epigenetic, and ultrastructural aspects is key to advance our understanding of the complex process of seed germination (Steinbrecher and Leubner-Metzger 2018).

We previously reported that *T. catharinensis* ripe cypsela structure includes the pericarp (exocarp), seed coat (exotesta), and endosperm surrounding the embryo (Elias et al. 2019). In addition, we studied the effects of abscisic acid (ABA) and gibberellic acid (GA_3) and their inhibitors, fluridone (FLU) and (PAC) at phase II of *T. catharinensis* seed germination (Lando et al. 2020). We observed 32 proteins differentially accumulated and that 69.66% of differentially accumulated proteins occurred as a result of the contrasting effects of GA_3 and ABA, and their inhibitors, PAC and FLU. Our hypothesis is that *T. catharinensis* seed the radicle protrusion occurs as a result of cell division and elongation of hypocotyl radicle axis. To understand this process, we studied cell cycle activity and the dynamics of global DNA methylation (GDM) variation, considering three phases of seed germination, in response to the exogenous application of GA_3, ABA, and their inhibitors PAC and FLU. Also, we analyze the chromatin ultrastructure in mature seeds and in phase II of seed germination.

Material and methods

Plant material

Seeds of *T. catharinensis* were collected in two natural populations located in Curitibanos, Santa Catarina, Brazil (latitude 27° 18′ S, longitude 50° 38′ W, altitude 990 m; latitude 27° 36′ S, longitude 48° 27′ W, altitude 930 m). Damaged seeds were removed by hand-sorting and the selected ones were kept in the fridge (8 ºC) for no more than 30 days, until the experiments were started. One specimen was stored in Flor Herbarium (UFSC- Brazil) under registration number FLOWER 38056.

Seed imbibition and germination

Seeds were immersed in ethanol 70% (v/v) for 1 min and disinfected in sodium hypochlorite (1% v/v) for 5 min. After that, the seeds were submitted to three washes in sterile distilled water. Immediately, eight replicates of 25 seeds were placed in a germination box with germitest paper moistened with 2.5 g of water per gram of paper. The seeds were weighed before imbibition, at 30-min intervals for 6 h, 1 h intervals up to 12 h, every 12 h up to 6 days, and finally, 24 h intervals until 50% of the seeds showed radicle protrusion. The percentage of mass increment (I) over time, as a function of initial seed mass (Justo et al. 2007), was calculated as $(I\ \%) = [(Mt - Mi)/Mi] \times 100$, where Mi = initial fresh mass of the sample, and Mt = mass sample at time of collection (t). The seeds were inoculated in germination boxes, under germitest paper moistened with 10 mL of solutions of GA_3, ABA and their respective PAC and FLU inhibitors (200 µM). In the treatment H_2O (control) was moistened with sterilized distilled water. All treatments were placed in a growth chamber at 20 ± 2 °C and photoperiod of 10 h light/14 h dark.

Morphological analyses

Seed samples were collected during germination and analyzed in a Leica EZ4 HD stereo microscope equipped with the Leica EZ4 image capture and Leica LAS EZ software.

Light microscopy

Samples were collected in the three phases of germination and were fixed in phosphate buffer 0.1 M (pH 7.2) containing 2.5% formaldehyde at room temperature for 48 h, according to Schmidt et al. (2009), with modifications. Subsequently, the samples were dehydrated. The samples were infiltrated with Historesin (Leica Historesin, Heidelberg, Germany) and cut into semi-thin sections (4 µm). Sections were stained with toluidine blue (TB-O) (O'Brien et al. 1964). Light microscopy (LM) sections were analyzed in a Leica DM2500 microscope equipped with the OPT 5.1 MP scientific camera and OPTHD software.

Transmission electron microscopy (TEM)

Samples were collected in the three phases of germination and were fixed in 0.1 M sodium cacodylate buffer (pH 7.2) containing 2.5% glutaraldehyde for 48 h, according to Schmidt et al. (2009), with modifications. The material was post-fixed with 0.1 M sodium cacodylate buffer containing 1% osmium tetroxide for 5 h, dehydrated in an increasing series of acetone aqueous solutions, and then embedded in Spurr's resin (Spurr 1969). Ultra-thin sections (60 nm) were collected on grids and stained with aqueous uranyl acetate followed by lead citrate. Three grids for each treatment were then examined in the JEM 1011 TEM (JEOL Ltda., Tokyo, Japan) at 80 kV.

Genomic DNA extraction and HPLC analysis of global DNA methylation

For the Global DNA methylation analysis, seeds were imbibed in the exogenous solutions of hormones GA_3 (200 µM) and ABA (200 µM) and their respective biosynthetic inhibitors, PAC and FLU (200 µM) (Sigma-Aldrich) and H_2O. In all treatments, samples were collected in Phase I (18–22 h of imbibition), phase II (72–75 h of imbibition) and phase III (radicle protrusion, 1 mm length) to according Figure S1 and were based on previous experiments performed at least three times. For treatments with no germination, samples from phase III were collected at 30 days (720 h), along with the control treatment (H2O). Radicle protrusion was considered the moment of seed germination. Four replicates with 40 embryos (after removal of the seed coat) each were evaluated in all treatments. DNA was extracted according to Doyle and Doyle (1987), with minor modifications. Briefly, frozen samples were ground into a fine powder with liquid nitrogen. Extraction buffer was composed of 2% CTAB, 1.4 M NaCl, 20 mM EDTA, 100 mM Tris–HCl, pH 8.0, 2% polyvinylpyrrolidone and 3% 2-mercaptoethanol. The re-extraction buffer was composed of 50 µL of 10% CTAB and 1.4 M NaCl. The extracted DNA was precipitated at − 80 °C with 2/3 volume of isopropanol by a period of 4 h. The DNA pellet was washed twice in 70% ethanol and once in 95% ethanol and then dried at ambient temperature followed by dissolution in 100 µL of water. Nucleid acids were quantified in a spectrophotometer Nanodrop 1000 (NanoDrop Technologies, Inc.). Digestion procedures were performed according to Johnston et al. (2005) and Fraga et al. (2012). Briefly, 100 µL of nucleic acids (1 µg μL^{-1}) were incubated for 5 min at 65 °C and then for 10 min at 4 °C. Subsequently, 10 µL of RNase A (10 µg μL^{-1}, Sigma-Aldrich) and 10 µL of RNase T1 (20 µg μL^{-1}, Sigma-Aldrich) were added and incubated for 17 h at 37 °C. Then, 20 µL of sodium acetate (3 M, pH 5.4) was added. DNA and RNA resistant to RNase were precipitated at − 20 °C with 136 µL of cold isopropanol for 30 min. Pellets were dried at ambient temperature and re-suspended in 100 µL of ultrapure water. The DNA concentration was adjusted to 0.25 µg μL^{-1}. Finally, DNA samples was digested with 10 µL of nuclease P1 (1.0 U mL^{-1} in 30 mM NaOAc, pH 5.4, Sigma-Aldrich) for 17 h at 37 °C. Then, 10 µL of 0.5 M Tris–HCl (pH 8.3) and 10 µL of alkaline phosphatase (10 U mL^{-1} $(NH4)_2SO_4$ 2.5 M, Sigma-Aldrich) were added and incubated for 2 h at 37 °C. The supernatant was collected and stored at − 20 °C until HPLC analysis. HPLC analysis was performed according to Johnston et al. (2005). A HyperClone™ 5 µm ODS (C18) 120 Å, LC Column 250 × 4.6 mm (Phenomenex, Torrance, USA), guard column (4.0 × 3.0 mm) (Phenomenex), and UV detector (280 nm) were used. The gradient program consisted of 3 min with 100% buffer A (0.5% v/v methanol in 10 mM KH_2PO_4 adjusted to pH 3.7 with phosphoric acid, 0.22 µm filtered), followed by a linear gradient from 3 to 20 min to 100% of buffer B (10% v/v methanol in 10 mM KH_2PO_4 adjusted to pH 3.7 with phosphoric acid, 0.22 µm filtered), followed by 20–25 min with 100% of buffer B. A flow rate of 1 mL min^{-1} and 20 µL of sample injection volume were applied. The dNTPs (Fermentas, Hanover, MD, USA) used as standards (dA, dT, dC and dG) and 5mdC were digested for 2 h with alkaline phosphatase (10 U mL^{-1}) and Tris–HCl (0.5 M, pH 8.3) at 37 °C to obtain the nucleosides. The standard nucleosides (5–50 mM) were prepared in deionized H_2O and stored at − 20 °C. 5mdC quantification (%) was performed according to 5mdC concentration divided by 5mdC concentration plus dC concentration multiplied by 100. The obtained peak area was analyzed by LC Solution software (Shimadzu, Kyoto, Japan). Data were analyzed by "R" statistical program (Team and Others 2013) and submitted to ANOVA. Treatments were compared by Student–Newman–Keuls (SNK) post hoc test ($p < 0.05$).

Flow cytometry

To flow cytometry (FC) analyses, the embryos were dissected into the radicle after 150 h of imbibition in the

exogenous solutions (GA_3, FLU, ABA, PAC) and H_2O. The true seed was removed from the pericarp, and the distal part of the radicle about 0.3–0.5 mm long, was cut off and used for flow cytometry. Four replicates containing six radicle tips were performed. Samples were prepared as described previously by (Rewers and Sliwinska 2014), with modifications. Plant tissue was cut with a sharp razor blade in a plastic Petri dish with 1 mL nucleus-isolation buffer (100 mM Tris, 2.5 mM MgCl2·6H_2O, 85 mM NaCl, 0.1% Triton X-100; 2% PVP, pH 7.0). After cutting, the suspension was passed through a 50 µm mesh nylon filter and added Propidium iodide and RNase (50 µg mL^{-1}) for DNA staining. For each sample, the fluorescence of 10,000 nuclei was analyzed using a FACSCanto II (BD Biosciences™, USA) flow cytometer. Analyses on four replicates. Histograms were analyzed using a Flowing Software 2.5.1, and the percentage of nuclei with different DNA contents were calculated. Treatments were compared by Student–Newman–Keuls (SNK) post hoc test ($p < 0.05$).

Results and discussion

Exotesta and endosperm rupture are sequential events during the seed germination of *Trichocline catharinensis* and includes cell division and ultrastructural changes.

Morphological and light microscopy (LM) observations showed modifications in hypocotyl-radicle axis (HRA) after imbibition in the treatment control—H_2O. In phase II, the hypocotyl-radicle axis showed a color change and a small elongation of this region (Fig. 1a). Also, evident intercellular spaces in the region of the fundamental meristem (later called the cortex) (Fig. 1b arrows). According to Evert (2006), intercellular spaces extend into meristematic tissues, where the dividing cells are respirating heavily. This was confirmed when we observed, in the outer layers of the pericycle (p), an endodermal layer (1) that divides periclinally (in a longitudinal orientation), giving rise to a new layer of the fundamental meristem (2) (Fig. 1b, c). This is also described at the Arabidopsis root apex (Dolan et al. 1993).

Furthemore, in the phase II the HRA has a size increase (Fig. 1d), corresponding to the beginning of micropylar endosperm (me) degradation and weakening. In the me region was observed pectic substances by the differentiated staining purplish blue with the use of TB-O (Fig. 1e). At the same time, the cells region of exotesta (ex), already showed evidence of rupture (Fig. 1e). According to Müller et al. (2006) and Yan et al. (2014) upon imbibition, after testa rupture of Nicotiana and Lactuca seeds, mannans are degraded in the micropylar endosperm. It already known that the endosperm cell walls have a diverse structure and compositions including hemicellulose and pectin monomers (Lee et al. 2012). In addition, cell wall remodeling enzymes (CWREs) are important for synthesizing, loosening and reinforcing the cell walls (Müller et al. 2006; Yan et al. 2014). Both the composition and abundance of CWREs alter the tensile properties that allow tissue to rupture (Lee et al. 2012). The signaling pathways of hormones GA and ABA which controls seed germination, through weakening of endosperm and expansion of embryo cell (Miransari and Smith 2014). The mechanism effects of excess ABA on embryo expansion, which inhibit the promoting effects of gibberellins on radicle growth, and hence it will not germinate through the endosperm and testa (Nonogaki 2017).

In phase III, in the seeds imbibed in H_2O, we observed morphologically the radicle protrusion through the endosperm (Fig. 1f). The light microscopy study showed three vacuolated and collapsed cell layers in the micropylar endosperm (me) (Fig. 1g detail), culminating with the rupture of endosperm and exotesta (Fig. 1h). The endospermic hole observed in Trichocline are also present in *Nicotiana tabacum* seeds; the radicle emerges through it and has a smooth outline. This endospermic hole always forms at the micropylar end and results from the degradation of the endosperm cells (Steinbrecher and Leubner-Metzger 2018). The rupture of the endosperm is a limiting process of germination, observed in sp. Asteraceae (Lactuca) and Solanaceae (Solanum, *N. tabacum*, Capsicum and Datura species), data reviewed by Steinbrecher and Leubner-Metzger (2017, 2018). These findings strongly suggest that endosperm and exotesta ruptures are sequential events as well crucial during phase III of the *T. catharinensis* seed germination.

During the germination stages in seeds imbibed with H_2O, we observed in the transmission electron microscopy (TEM) of the HRA showed cytoplasm change and organization. In phase I, we observed cells of HRA with protein storage vacuoles (PSVs), consisting of a crystalloid matrix and small lytic vacuoles (LV) (Fig. 2a). PSVs initiate the proteolysis, by the fusion of the LV (Fig. 2b, c). The cells showed cytoplasm with a large number of free ribosomes (Fig. 2b arrowhead) or clusters (polyribosomes) (Fig. 2d detail), rough endoplasmic reticulum (RER), mitochondria and Golgi (G) (Fig. 2c–e detail). These characteristics are indicative of a possible onset of protein synthesis. It seems that ribosomal activity increases dramatically during imbibition, facilitating the synthesis of new proteins for seed germination (Lando et al. 2020). Upon seed imbibition, a metabolic switch happens and the metabolites accumulated during seed maturation are consumed by being mobilized and/or degraded, also with that, germination-associated gene expression programs already start during seed imbibition (Derek Bewley et al. 2012; Obroucheva et al. 2017). We observed intracellular traffic via plasmodesmata (Fig. 2b

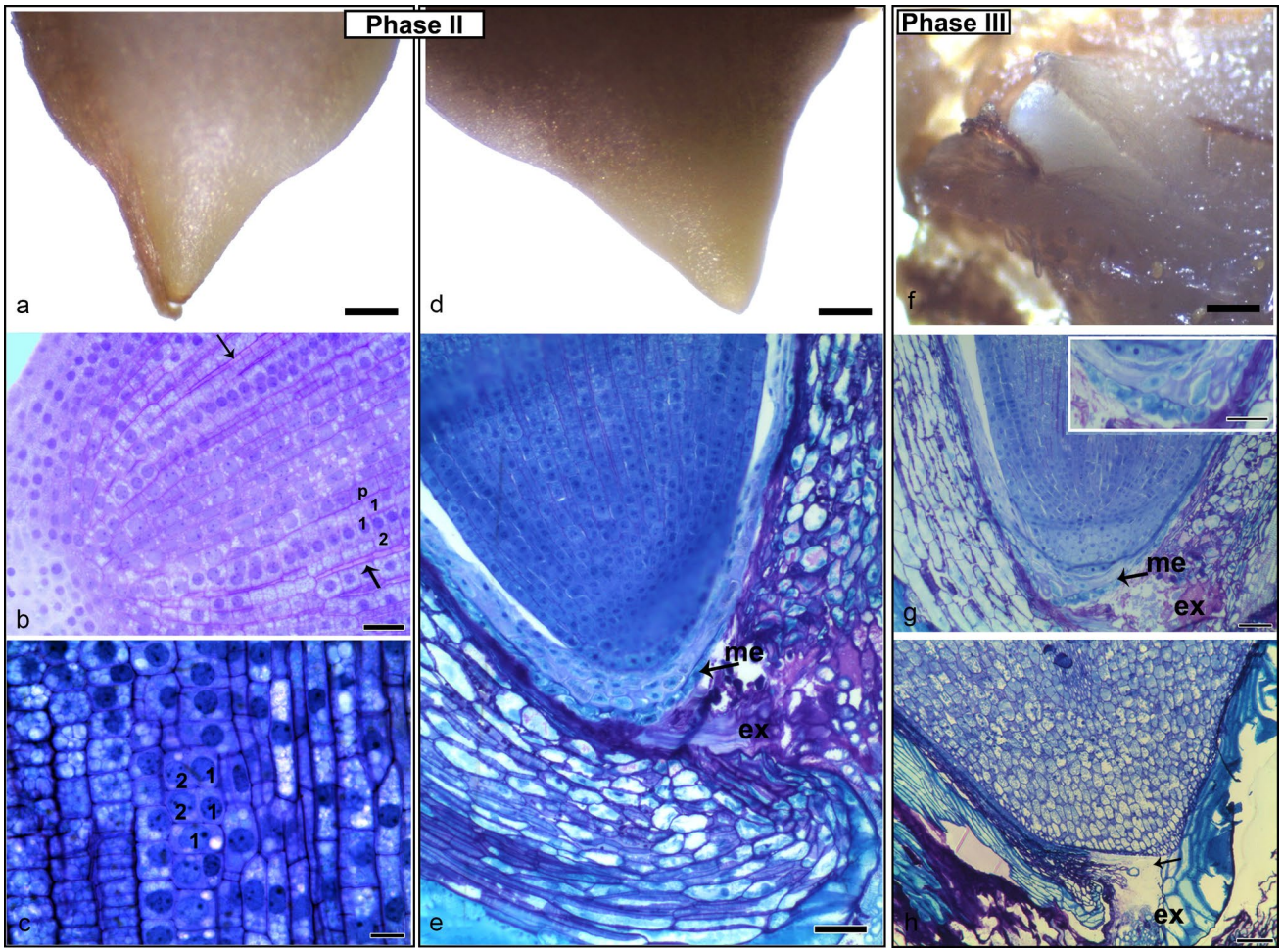

Fig. 1 Morpho-histological observations of the seed germination of *T. catharinensis* imbibed in H_2O. **a** Phase II: Hypocotyl-radicle axis (HRA) color change and a small elongation of this region; **b** the longitudinal section of HRA in light microscopy showed intercellular spaces evident in the region of the fundamental meristem (arrows). In the outer layers of the pericycle (p), an endodermal layer (1) divides periclinal (in a longitudinal orientation), giving rise to a new layer of the fundamental meristem (2); **c** details of layers of the pericycle (p), an endodermal layer (1) divides periclinal (in a longitudinal orientation), giving rise to a new layer of the fundamental meristem (2); **d** phase II: hypocotyl-radicle axis has a size increase; **e** longitudinal section showed micropylar endosperm (arrow) degradation to promote endosperm weakening. In this region the accumulation of pectic substances was evidenced, proved by the differentiated staining with the use of TB-O, also in exotesta (ex); **f** phase III: the radicle protrusion by the endosperm; **g** the longitudinal section showed three cell layers of the micropylar endosperm (me) and vacuolated and collapsed, showed accumulation of pectic substances (detail); **h** The loosening of endosperm cells, allow tissue to rupture causing an opening at the micropylar end (arrow). Scale bars = **a**; **d**; **f**. 0.5 mm. **b**; **g** detail 25 µm. **c** 10 µm. **e**; **h**. 50 µm

arrows) indicating that the metabolism is being initiated and activated.

In phase II, seems to have a change in proportion of LV in PSVs in HRA cells (Fig. 2f), however the quantification was not performed by MET analysis. This mobilization, as noted, does not occur simultaneously in all cells (Fig. 2g, h). The PSVs presented several stages of degradation, according to the LV fusion. The lipid bodies (LBs), remained around the PSVs. More intercellular spaces were observed in phase II compared to phase I (Fig. 2f asterisk). Nucleus showed nucleolus (NU) with heterochromatin (arrowhead) and euchromatin (arrow) distinct (Fig. 2h). According to Obroucheva et al. (2012) an additional increase of the water content in phase III is required for the onset of growth in the embryonic axes. We also observed that the intercellular spaces were maintained in phase III (Fig. 2i, j asterisk). The PSVs underwent dedifferentiation of the crystalloid matrix and coalescence of the LV, causing the formation of a central vacuole, occupying a large part of the cytoplasm (Fig. 2i, j). The organelles M, Golgi, glyoxysomes (GL) and RER were reduced to one layer, close to the cell membrane (Fig. 2k). In this phase, the vacuoles (v) are full of fibrillar material and small membrane fragments, due to the numerous fusions and intravacuolar digests related to the mobilization of the

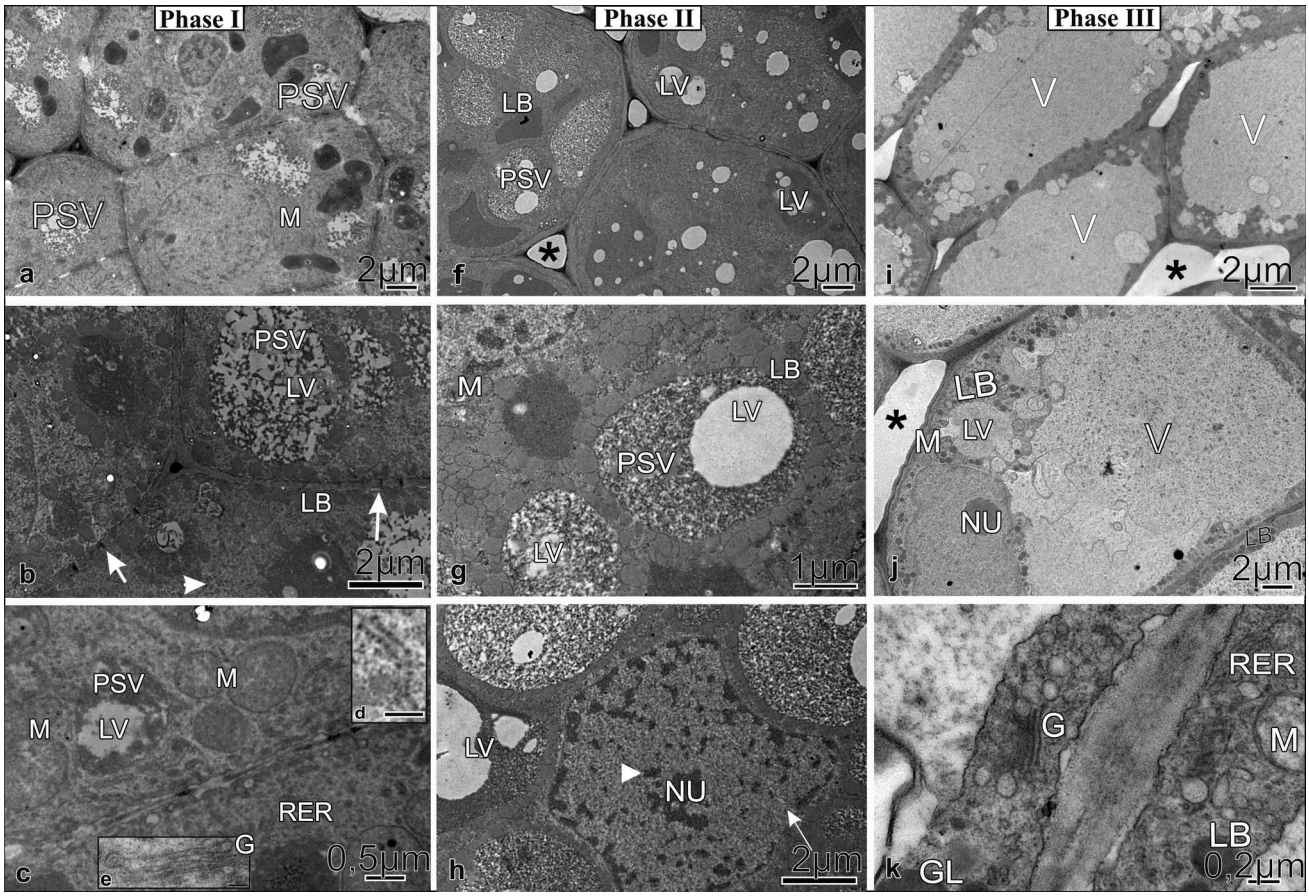

Fig. 2 Transmission electron microscopy analysis of hypocotyl-radicle axis (HRA) cells during germination of *T. catharinensis* seeds in the H_2O: phase I—**a** cells with protein storage vacuoles (PSVs), consisting of a crystalloid matrix and small lytic vacuoles (LV); **b** PSVs initiate the proteolysis, by the fusion of the LV. Presence of lipid bodies (LB) near the cell membrane and around the PSVs. plasmodesmata in the cell wall (arrows). Free ribosomes were observed in the cytoplasm (arrowhead); **c** mitochondria (M) and rough endoplasmic reticulum (RER); **d** detail polyribosomes; **e** detail golgi (G); Phase II—**f** The PSVs presented several stages of degradation, according to the LV fusion. intercellular spaces (asterisk); **g** LBs around PSVs; **h** Nucleus showed nucleolus (NU) with heterochromatin (arrowhead) and euchromatin (arrow) distinct; **Phase III**- **l** formation of a central vacuole, occupying a large part of the cytoplasm; **j** coalescence of the LV with central vacuole; **k** Organelles close to cell membrane—Golgi (G), glyoxysomes (GL), rough endoplasmic reticulum (RER), mitochondria (M). Also, close to cell membrane lipid bodies (LB)

reserves (Fig. 2i, j). According to Zheng and Staehelin (2011), in cortex cells of *N. tabacum* radicle, lytic vacuoles are formed by a process involving PSV fusion, storage protein degradation and the gradual substitution of intrinsic α-tonoplast protein (TIP) of the PSV with the γ-TIP lytic vacuole (LV) marker protein. This aqueous lytic vacuolar compartment has to be formed to provide turgidity pressure, directing cell elongation to promote radicle protrusion (Maeshima et al. 1994; Inoue et al. 1995). Protein storage vacuoles for lytic vacuoles occur clearly prior to the initiation of cell elongation at the elongation zone of the radicle (Novikova et al. 2014). Plant cells adjust the extensibility of cell walls by remodeling major wall components, cellulose microfibrils and /or pectin/hemicellulose matrix (Schopfer and Plachy 1984). Cell wall acidification increases by membrane H + ATPase and results in the activation of some cell wall enzymes, in particular xyloglucan endotransglicosylase (XET), methyl esterase and expansins. Expansins are proteins that interrupt the hydrogen bonds between cellulose and hemicelluloses. Thus, the mechanism of "acid growth" begins to operate and prepare the cells for the elongation at the end of the germination (Novikova et al. 2014). We observed mobilization of the lipid reserves, evidenced by the lower relative volume of (LB) that were closer to the membrane (Fig. 2k). Reserves are mobilized, and converted into easily transportable low molecular weight metabolites into growing regions, in support of the energy production (Derek Bewley et al. 2012).

In addition to the micropylar endosperm rupture and hypocotyl-radicle axis elongation observed by cell changes, we also observed the onset of cell division in *T. catharinensis* seeds. Flow cytometric histograms from embryonic

nuclei after 150 h imbibition in H_2O, showed one large peak, corresponding to the 2C DNA content (G1 phase of the cell cycle), and the second smaller peak, corresponding to nuclei with replicated 4C DNA content (G2 phase) (Fig. 3a). The most commonly accepted view is that the initiation of DNA synthesis leading to mitotic activity only contributes to post-germination root growth (Sliwinska et al. 2009; Derek Bewley et al. 2012). However, in some species such as *N. tabacum,* Solanum and Arabidopsis, cell division was detected before protrusion of the radicle (de Castro et al. 2000; Masubelele et al. 2005). To better understand the activity of the cell cycle and in order to gain insight associated with germination of seeds, we applied GA_3, ABA and their PAC and FLU inhibitors, the relative abundance of these hormones constitutes a metabolic threshold mechanism that regulates the germination process (Weitbrecht et al. 2011). Flow cytometric histograms in response of GA_3, ABA and their inhibitors PAC and FLU, after 150 h of imbibition, also showed one large peak, corresponding to the 2C DNA content (G1 phase of the cell cycle), and the second smaller peak, corresponding to nuclei with replicated 4C DNA content (G2 phase) as observed in seeds imbibition in H_2O (Fig. 3a–e). We observed that the percentage of nuclei with 4C DNA is higher significantly in seeds embedded in FLU, GA_3 and H_2O. In these treatments there is no delay in germination, as observed in the imbibition curve (Fig. 4a–c). At the end of phase II, there is an increase in uptake water and the start of phase III. We observed that more than 80% of the nuclei were in the G0/G1 phase of the cell cycle (having 2C DNA), and there were no more than 12% of 4C (G2) nuclei (Fig. 4f). These results strongly suggest that there is no endopolyploidization in *Trichocline* HRA cells which is similar to the *Helianthus annuus* species, also an Asteraceae, which probably completed germination due to cell division (Rewers and Sliwinska 2014).

Global DNA Methylation levels are affected by GA_3, ABA and their inhibitors during the germination of *T.catharinensis* seeds

Epigenetic mechanisms involving global DNA methylation (GDM) and chromatin modifications occur in the regulation of gene expression and adjustment of physiological activities (Arikan et al. 2018), and it is likely that GDM is involved in the condensation and decondensation of chromatin during maturation and seed germination, respectively (Bartels et al. 2018). The change from one stage (dry seed) to germination (metabolically active state) requires significant changes in the spatial and temporal patterns of gene expression (Wolny et al. 2017). Generally, seed germination could be divided into three phases based on the style of water uptaking (Fig. 4) (Derek Bewley et al. 2012) associated the

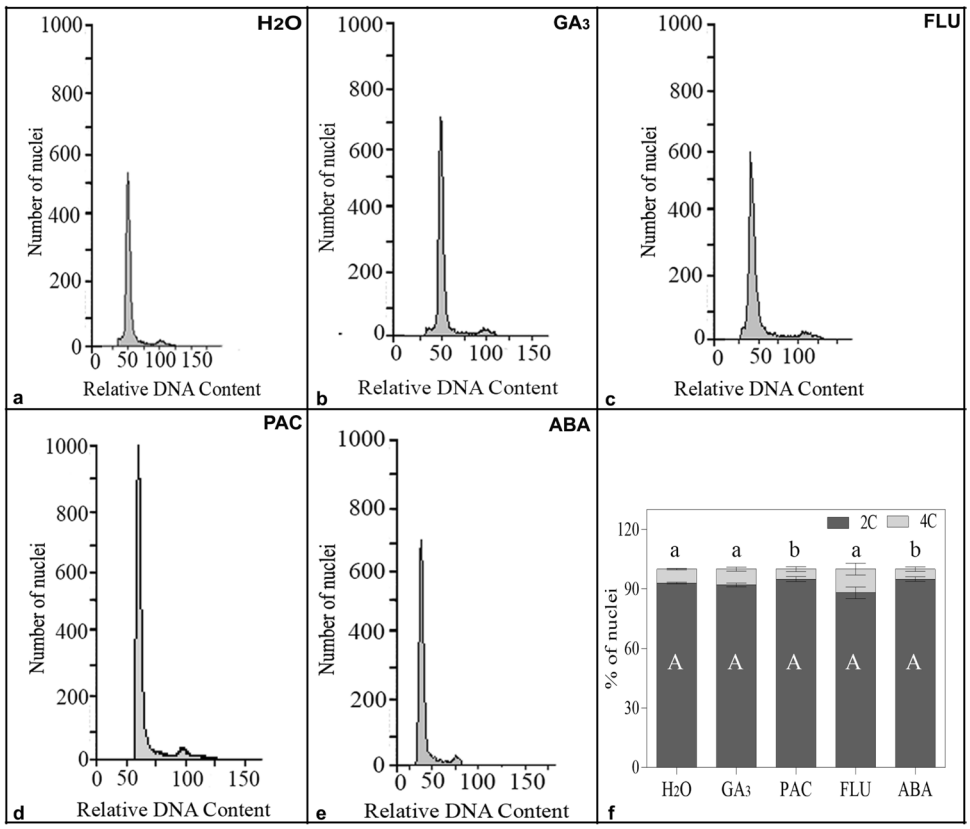

Fig. 3 Flow cytometric analysis of the cell cycle activity from hypocotyl-radicle axis of *Trichocline catharinensis* embryo after 150 h of seed imbibition in exogenous solutions: **a** H_2O; **b** GA_3; **c** FLU; **d** PAC; **e** ABA; **f** proportion of nuclei with different DNA contents in H_2O, GA_3, FLU, PAC, ABA ($n=4$); $p<0.05$, two-way ANOVA with SNK test

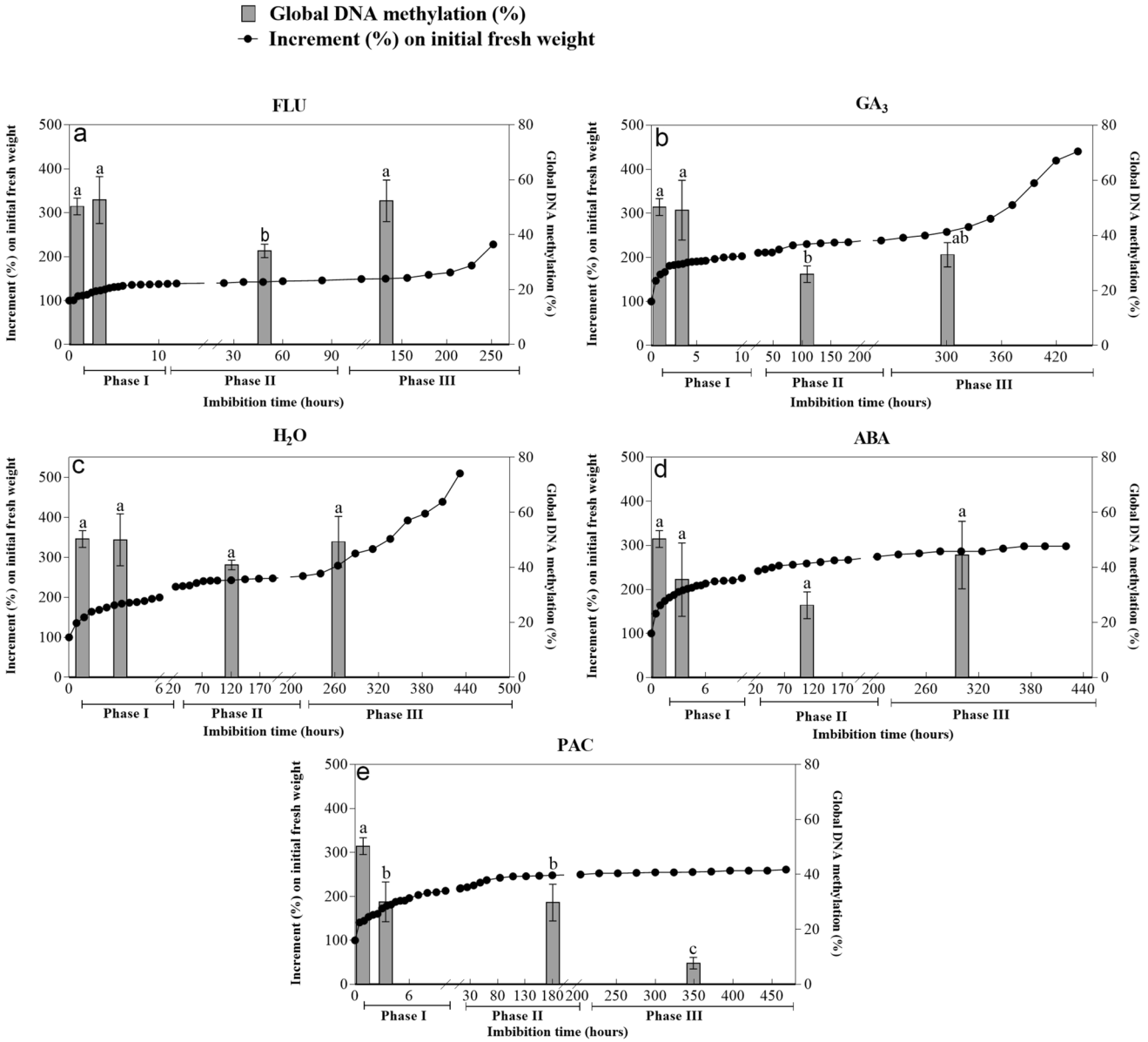

Fig. 4 Dynamics of global DNA methylation of *T. catharinensis* seed and mass increment in the three phases of germination (I, II and III) under exogenous solutions of fluridone FLU (**a**); gibberellin GA_3 (**b**); water H_2O (**c**); abscisic acid ABA (**d**); paclobutrazol PAC (**e**). Data mean ± SD ($n = 4$). Means followed by the same letter are not significantly different by the SNK test ($p < 0.05$)

germination phases, GDM and chromatin structure undergoes dynamic reprogramming events (Kawakatsu et al. 2017).

In the present study, we revealed an interesting connection between GDM and change in the organization of chromatin at the ultrastructural level with the promotion or inhibition of germination. We observed that the mature seed had a higher level of GDM (50%), associated with higher chromatin compaction (heterochromatin) (Figs. 4c, 5a). In the dry seeds, GDM is concentrated on chromocenters (more compacted regions), which in TEM appear more electron-dense (van Zanten et al. 2011). These results are possibly related to desiccation tolerance, since in orthodox seeds an increase in GDM may allow them to survive storage and desiccation, the condensation of chromatin, which increases genomic stability and silences DNA transcription, is assisted by DNA methylation and other epigenetic modifications (Feser and Tyler 2011). Similar results were also observed by Kawakatsu et al. (2017), Meng et al. (2012) and Van Zanten et al. (2011).

In all treatments, in the Phase II, GDM levels decreased possibly related to metabolic activities and transcriptional activation, initiated by the germination process (Fig. 4a–e). Furthermore, the coincidence of DNA demethylation with

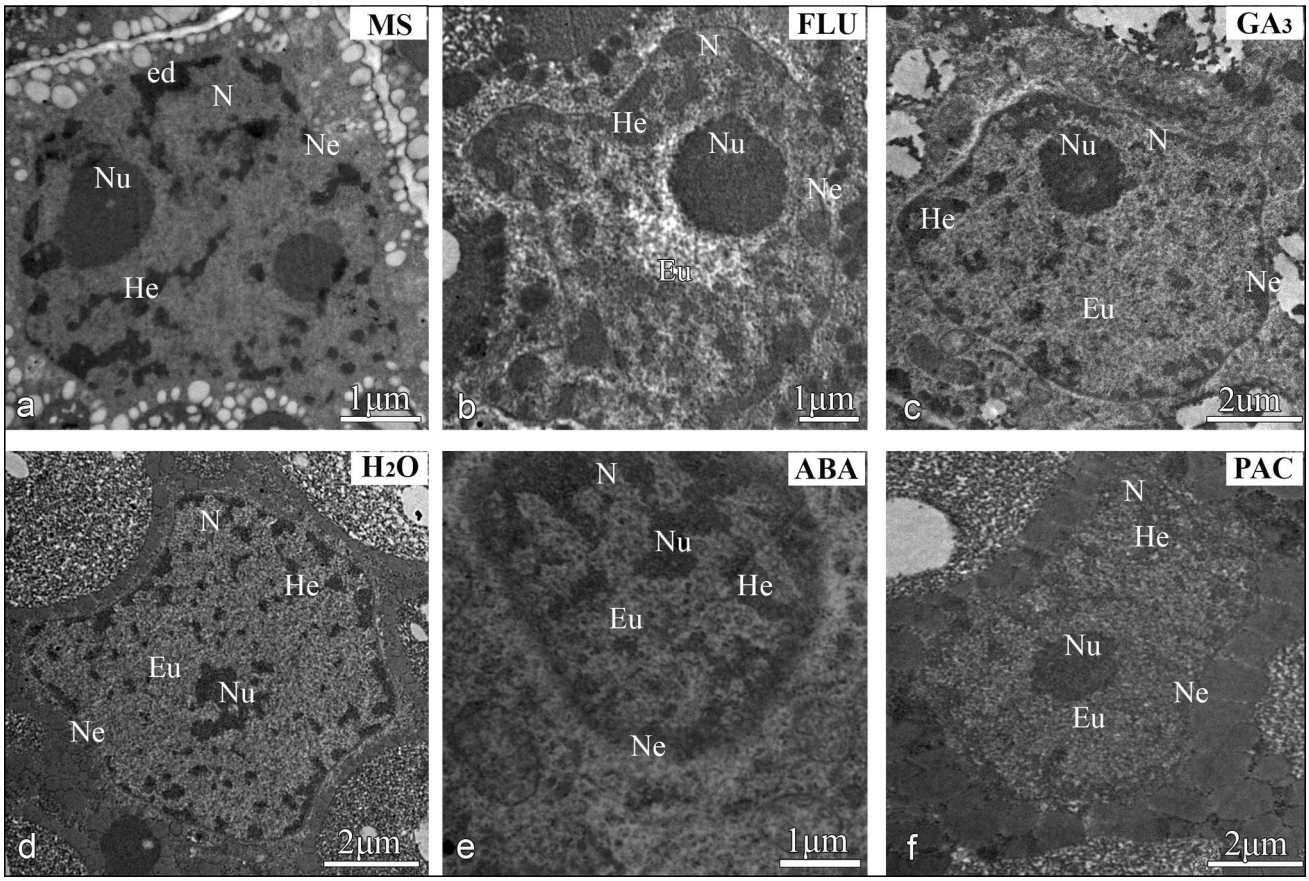

Fig. 5 Ultrastructural characterization of *T. catharinensis* embryo cells by TEM analysis, showed cells with nuclei (N), nucleolus (Nu) showing euchromatin (Eu) and heterochromatin (He) regions near the periphery of the nuclear envelope (Ne) more electron-dense (Ed) **a** mature seed; **b** cells imbibed-FL; **c** cells imbibed-GA_3; **d** cells imbibed-H_2O; **e** cells imbibed-ABA; **f** cells imbibed-PAC; FLU: fluridone; GA_3: gibberellin; H_2O: water; ABA: abscisic acid; PAC: paclobutrazol

the onset of DNA replication in cells of the seed (Nonogaki 2010) argues for a mechanism of passive demethylation rather than active demethylation (Narsai et al. 2017). In addition, TEM analyses showed the nucleus of the cells, after 75 h of imbibition, with decondensed chromatin (regions of euchromatin Eu) and without electron-dense regions in comparison to dry seed (Fig. 5b–f). It was reported that the changes in chromatin organization are accompanied by changes in the spatial distribution of methylated DNA sequences (van Zanten et al. 2011). This is in line with previous reports showing that the global DNA methylation declines during germination (Meng et al. 2012; Bräutigam et al. 2013; van Zanten et al. 2013). In the treatments FLU and GA_3, it was observed a significantly reduction of GDM compared to H_2O in phase II (Fig. 4). According to Manoharlal et al. (2018) the GA_3 application induced a similar declining trend in global DNA methylation during tobacco vegetative growth. It seems like GA_3 may have an indirect effect on DNA methylation by increasing the mobility and/or modification of linker histones (H1 and its variants) as was reported by Wierzbicki and Jerzmanowski (2005).

However, at phase III of seed germination, we observed significant differences in the level of GDM in the treatment with PAC in relation of others. The exogenous PAC resulted in a gradual reduction in GDM levels from 29% in phase II to 7% in phase III (Fig. 4e). Moreover, the structure of the chromatin in TEM images after 75 h of imbibition in PAC is decondensed (Fig. 5f). PAC treatment, by inhibiting germination, can resulted in decreased levels of methylation (Peng and Zhang 2009). Several reports have demonstrated that global demethylation can affect genome integrity and gene regulation (Koji et al. 2009; Anderson et al. 2009; Shimoda et al. 2014). The germination-associated gene regulation programs already start during seed imbibition (Narsai et al. 2017; Malabarba et al. 2021). Recent studies have shown that PAC-imbibed seeds remained at phase II, by halted reserve mobilization (Lando et al. 2020). Therefore, the cell division and cell elongation are arrested, it suggests

that DNA replication is also stopped, caused decreased of DNA methylation.

However, in the treatments in H_2O, FLU, and GA_3 in phase III, there is an increased in GDM which reaches a level similar to Phase I (Fig. 4). These results might be associated to chromatin reorganization in order to the new transcription program for cell division and elongation during the phases of process germination. The regulation of gene expression is not limited to the promoter region, but can be achieved by changing the methylation status of the coding region, leading to a differentiated expression of genes or deletion in the expression of genes related to germination (Peng and Zhang 2009; Suriyasak et al. 2021). The results observed in our study suggest the involvement of DNA methylation in the seed germination of *T. catharinensis* seeds, possibly a passive demethylation when the mobilization of reserves altered gene regulation and promoted cell division and elongation. What we don't observe with PAC, inhibitor of seed germination. To better elucidate these mechanisms, further studies are needed.

Conclusions

In conclusion, our results showed that *Trichocline* seeds germination occurs with the protrusion of radicle trough of endosperm rupture and exotesta are sequential events. The observed HRA cell elongation during germination is accompanied by the enlargement of vacuoles due to the transformation of protein storage vacuoles. Together with elongation of the HRA cells, the replication to 4C DNA content (G2 phase of cycle cellular) occurs as is before to complete the germination. We also suggest that this is related to the reduction of levels of GDM observed in the phase II, after 72 h of imbibition, when DNA replication is possibly initiated. In the seeds imbibed FLU, GA_3 and H_2O, showed higher numbers of cells with nuclei 4C DNA. However, when we applied the PAC, an inhibitor of GA_3 synthesis, we observed the levels of GDM decrease dramatically in phase III. In addition, there is no fresh weight (FW) increase at this phase because germination is inhibited. In the mature seed we observed compacted chromatin in electron-dense regions (heterochromatin), becoming loosened during germination in regions of euchromatin. As we observed, there are few seed studies that correlate ultrastructural changes with molecular processes before the protrusion of the radicle. This information brings insights into fundamental processes involved in seed germination that may be useful in agronomically important practices, such as seed priming, as well to promote the conservation of germplasm of wild species.

Supplementary Information The online version contains supplementary material available at https://doi.org/10.1007/s11738-024-03663-7.

Acknowledgements The authors thank the staff of the Central Laboratory of Electron Microscopy (LCME/Brazil), to Plant Developmental Physiology and Genetics Laboratory of the Federal University of Santa Catarina (LFDGV/Brazil), to Multiuser Laboratory of Biology Studies (LAMEB/Brazil). We also thank the Laboratory of Plant Anatomy (LAVEG/Brazil). We thank Prof. Elwira Sliwinska of the Laboratory of Molecular Biology and Cytometry of the University of Science and Technology (Poland) for the important contributions in the analysis of flow cytometry. This article is part of the PhD Thesis of Ana Paula Lando at Federal University of Santa Catarina. A copy of Ph.D. Thesis is deposited on line: https://repositorio.ufsc.br/bitstream/handle/123456789/211598/PRGV0294-T.pdf?sequence=-1&isAllowed=y.

Author contributions APL and NS conceived and designed the research. APL, DG, WGV, YF performed the experiments. APL, WGV, NS analyzed the data. APL and NS wrote the manuscript. All the authors have read and approved the manuscript.

Funding This work was supported by the Conselho Nacional de Desenvolvimento Científico e Tecnológico (CNPq, Brazil) and Coordenação de Aperfeiçoamento de Pessoal de Nível Superior (CAPES, Brazil). Grant Number of Neusa Steiner (311156/2017-7 457940/2014-0).

Declarations

Conflict of interest The authors declare that there is no conflict of interest.

References

Anderson RM, Bosch JA, Goll MG et al (2009) Loss of Dnmt1 catalytic activity reveals multiple roles for DNA methylation during pancreas development and regeneration. Dev Biol 334:213–223

Arikan MK, Metin B, Tarhan N (2018) EEG gamma synchronization is associated with response to paroxetine treatment. J Affect Disord 235:114–116

Bartels A, Han Q, Nair P et al (2018) Dynamic DNA methylation in plant growth and development. Int J Mol Sci. https://doi.org/10.3390/ijms19072144

Bird A (2002) DNA methylation patterns and epigenetic memory. Genes Dev 16:6–21

Bräutigam K, Vining KJ, Lafon-Placette C et al (2013) Epigenetic regulation of adaptive responses of forest tree species to the environment. Ecol Evol 3:399–415

Cabrera AL, Klein RM, Reitz R (1973) Compostas: tribo: Mutisieae. Herbário 'Barbosa Rodrigues'

de Castro RD, van Lammeren AA, Groot SP et al (2000) Cell division and subsequent radicle protrusion in tomato seeds are inhibited by osmotic stress but DNA synthesis and formation of microtubular cytoskeleton are not. Plant Physiol 122:327–336

Derek Bewley J, Bradford K, Hilhorst H, Nonogaki H (2012) Seeds: physiology of development, germination and dormancy. Springer, Berlin

Dolan L, Janmaat K, Willemsen V et al (1993) Cellular organisation of the *Arabidopsis thaliana* root. Development 119:71–84

Doyle JJ, Doyle JL (1987) A rapid DNA isolation for small quantities of fresh leaf tissue. Phytochem Bull 19:11–15

Drozhdeniuk AP, Sulimova GE, Vaniushin BF (1976) Changes in base composition and molecular population of wheat DNA on germination. Mol Biol 10:1378–1386

Elias RA, Lando AP, Viana WG et al (2019) Structural aspects of cypsela and seed development of *Trichocline*

catharinensis (Cabrera): a Brazilian endemic species. Protoplasma 256:1495–1506
Engelmann F (2011) Cryopreservation of embryos: an overview. Methods Mol Biol 710:155–184
Evert RF (2006) Esau's plant anatomy: meristems, cells, and tissues of the plant body: their structure, function, and development. Wiley, New York
Feser J, Tyler J (2011) Chromatin structure as a mediator of aging. FEBS Lett 585:2041–2048
Fraga HPF, Vieira LN, Caprestano CA et al (2012) 5-Azacytidine combined with 2,4-D improves somatic embryogenesis of *Acca sellowiana* (O. Berg) Burret by means of changes in global DNA methylation levels. Plant Cell Rep 31:2165–2176
Inoue K, Motozaki A, Takeuchi Y et al (1995) Molecular characterization of proteins in protein-body membrane that disappear most rapidly during transformation of protein bodies into vacuoles. Plant J 7:235–243
Johnston JW, Harding K, Bremner DH et al (2005) HPLC analysis of plant DNA methylation: a study of critical methodological factors. Plant Physiol Biochem 43:844–853
Justo CF, Alvarenga AAD, Nery FC, Delu Filho N (2007) Chemical composition, imbibition curve and temperature effect on seed germination of *Eugenia pyriformis* Camb. (Myrtaceae). Revista Brasileira Biociências 5:510–512
Kawakatsu T, Nery JR, Castanon R, Ecker JR (2017) Dynamic DNA methylation reconfiguration during seed development and germination. Genome Biol 18:171
Koji T, Kondo S, Hishikawa Y et al (2009) In situ detection of methylated DNA by histo endonuclease-linked detection of methylated DNA sites: a new principle of analysis of DNA methylation. Histochem Cell Biol 131:165–165
Lando AP, Viana WG, Vale EM et al (2020) Cellular alteration and differential protein profile explain effects of GA3 and ABA and their inhibitor on *Trichocline catharinensis* (Asteraceae) seed germination. Physiol Plant 169:258–275
Lee KJD, Dekkers BJW, Steinbrecher T et al (2012) Distinct cell wall architectures in seed endosperms in representatives of the Brassicaceae and Solanaceae. Plant Physiol 160:1551–1566
Long RL, Gorecki MJ, Renton M et al (2015) The ecophysiology of seed persistence: a mechanistic view of the journey to germination or demise. Biol Rev Camb Philos Soc 90:31–59
Lukaszewska E, Virden R, Sliwinska E (2012) Hormonal control of endoreduplication in sugar beet (*Beta vulgaris* L.) seedlings growing in vitro. Plant Biol 14:216–222
Maeshima M, Hara-Nishimura I, Takeuchi Y, Nishimura M (1994) Accumulation of vacuolar H+-pyrophosphatase and H+-ATPase during reformation of the central vacuole in germinating pumpkin seeds. Plant Physiol 106:61–69
Malabarba J, Windels D, Xu W, Verdier J (2021) Regulation of DNA (de)methylation positively impacts seed germination during seed development under heat stress. Genes (basel) 457:12–23
Manning JC, Simka B, Boatwright JS, Magee AR (2016) A revised taxonomy of Gerbera sect. Gerbera (Asteraceae: Mutisieae). S Afr J Bot 104:142–157
Manoharlal R, Saiprasad GVS, Ullagaddi C, Kovařík A (2018) Gibberellin A3 as an epigenetic determinant of global DNA hypomethylation in tobacco. Biol Plant 62:11–23
Masubelele NH, Dewitte W, Menges M et al (2005) D-type cyclins activate division in the root apex to promote seed germination in Arabidopsis. Proc Natl Acad Sci U S A 102:15694–15699
Meng F-R, Li Y-C, Yin J et al (2012) Analysis of DNA methylation during the germination of wheat seeds. Biol Plant 56:269–275
Miransari M, Smith DL (2014) Plant hormones and seed germination. Environ Exp Bot 99:110–121
Müller K, Tintelnot S, Leubner-Metzger G (2006) Endosperm-limited Brassicaceae seed germination: abscisic acid inhibits embryo-induced endosperm weakening of *Lepidium sativum* (cress) and endosperm rupture of cress and *Arabidopsis thaliana*. Plant Cell Physiol 47:864–877
Narsai R, Gouil Q, Secco D, Srivastava A, Karpievitch YV, Liew LC, Lister R, Lewsey MG, Whelan J (2017) Extensive transcriptomic and epigenomic remodelling occurs during *Arabidopsis thaliana* germination. Genome Biol 172:15–18
Nonogaki H (2010) MicroRNA gene regulation cascades during early stages of plant development. Plant Cell Physiol 51:1840–1846
Nonogaki H (2017) Seed biology updates—highlights and new discoveries in seed dormancy and germination research. Front Plant Sci 8
Novikova GV, Tournaire-Roux C, Sinkevich IA et al (2014) Vacuolar biogenesis and aquaporin expression at early germination of broad bean seeds. Plant Physiol Biochem 82:123–132
O'Brien TP, Feder N, McCully ME (1964) Polychromatic staining of plant cell walls by toluidine blue O. Protoplasma 59:368–373
Obroucheva NV, Lityagina SV, Novikova GV, Sin'kevich IA (2012) Vacuolar status and water relations in embryonic axes of recalcitrant Aesculus hippocastanum seeds during stratification and early germination. AoB Plants 2012:ls008
Obroucheva NV, Sinkevich IA, Lityagina SV, Novikova GV (2017) Water relations in germinating seeds. Russ J Plant Physiol 64:625–633
Penfield S, MacGregor DR (2017) Effects of environmental variation during seed production on seed dormancy and germination. J Exp Bot 68:819–825
Peng H, Zhang J (2009) Plant genomic DNA methylation in response to stresses: potential applications and challenges in plant breeding. Prog Nat Sci 19:1037–1045
Piskurewicz U, Jikumaru Y, Kinoshita N et al (2008) The gibberellic acid signaling repressor RGL2 inhibits Arabidopsis seed germination by stimulating abscisic acid synthesis and ABI5 activity. Plant Cell 20:2729–2745
Rewers M, Sliwinska E (2014) Endoreduplication in the germinating embryo and young seedling is related to the type of seedling establishment but is not coupled with superoxide radical accumulation. J Exp Bot 65:4385–4396
Santos AP, Ferreira L, Maroco J, Oliveira MM (2011) Abiotic stress and induced DNA hypomethylation cause interphase chromatin structural changes in rice rDNA loci. Cytogenet Genome Res 132:297–303
Saracco F, Bino RJ, Bergervoet JHW, Lanteri S (1995) Influence of priming-induced nuclear replication activity on storability of pepper (*Capsicum annuum* L.) seed. Seed Sci Res 5:25–29
Schmidt EC, Scariot LA, Rover T, Bouzon ZL (2009) Changes in ultrastructure and histochemistry of two red macroalgae strains of *Kappaphycus alvarezii* (Rhodophyta, Gigartinales), as a consequence of ultraviolet B radiation exposure. Micron 40:860–869
Schopfer P, Plachy C (1984) Control of seed germination by abscisic acid. Plant Physiol 76:155–160
Shimoda N, Izawa T, Yoshizawa A et al (2014) Decrease in cytosine methylation at CpG island shores and increase in DNA fragmentation during zebrafish aging. Age 36:103–115
Sliwinska E, Bassel GW, Bewley JD (2009) Germination of *Arabidopsis thaliana* seeds is not completed as a result of elongation of the radicle but of the adjacent transition zone and lower hypocotyl. J Exp Bot 60:3587–3594
Spurr AR (1969) A low-viscosity epoxy resin embedding medium for electron microscopy. J Ultrastruct Res 26:31–43
Steinbrecher T, Leubner-Metzger G (2017) The biomechanics of seed germination. J Exp Bot 68:765–783
Steinbrecher T, Leubner-Metzger G (2018) Tissue and cellular mechanics of seeds. Curr Opin Genet Dev 51:1–10
Suriyasak C, Hatanaka K, Tanaka H, Okumura T, Yamashita D, Attri P, Koga K, Shiratani M, Hamaoka N, Ishibashi Y (2021) Alterations

of DNA methylation caused by cold plasma treatment restore delayed germination of heat-stressed rice (*Oryza sativa* L.) seeds. ACS Agric Sci Technol 1:5–10

Team RC et al (2013) R: a language and environment for statistical computing

van Zanten M, Koini MA, Geyer R et al (2011) Seed maturation in *Arabidopsis thaliana* is characterized by nuclear size reduction and increased chromatin condensation. Proc Natl Acad Sci USA 108:20219–20224

van Zanten M, Liu Y, Soppe WJJ (2013) Epigenetic signalling during the life of seeds. Epigenetic memory and control in plants, pp 127–153

Weitbrecht K, Müller K, Leubner-Metzger G (2011) First off the mark: early seed germination. J Exp Bot 62:3289–3309

Wierzbicki AT, Jerzmanowski A (2005) Suppression of histone H1 genes in Arabidopsis results in heritable developmental defects and stochastic changes in DNA methylation. Genetics 169:997–1008

Wolny E, Braszewska-Zalewska A, Kroczek D, Hasterok R (2017) Histone H3 and H4 acetylation patterns are more dynamic than those of DNA methylation in *Brachypodium distachyon* embryos during seed maturation and germination. Protoplasma 254:2045–2052

Yan D, Duermeyer L, Leoveanu C, Nambara E (2014) The functions of the endosperm during seed germination. Plant Cell Physiol 55:1521–1533

Zheng H, Staehelin LA (2011) Protein storage vacuoles are transformed into lytic vacuoles in root meristematic cells of germinating seedlings by multiple, cell type-specific mechanisms. Plant Physiol 155:2023–2035

Zluvova J, Janousek B, Vyskot B (2001) Immunohistochemical study of DNA methylation dynamics during plant development. J Exp Bot 52:2265–2273